COMPARISON OF REGULARIZATION METHODS FOR NUCLEON-NUCLEON EFFECTIVE FIELD THEORY

JAMES V. STEELE [a]
Department of Physics, Ohio State University
Columbus, OH 43210-1168

The characteristics of a meaningful effective field theory (EFT) analysis are discussed and compared with traditional approaches to NN scattering. A key feature of an EFT treatment is a systematic expansion in powers of momentum, which is demonstrated using an error analysis introduced by Lepage. A clear graphical determination of the radius of convergence for the momentum expansion is also obtained. I use these techniques to compare cutoff regularization, two forms of dimensional regularization, and the dibaryon approach, using a simple model for illustration. The naturalness of the parameters and predictions for other observables are also shown.

1 Introduction

An effective field theory (EFT) description of nucleon-nucleon (NN) scattering is an important step on the road to a consistent description of nuclear matter. It also provides the techniques to predict other observables such as bound state expectation values. However, the interaction of two heavy nucleons requires a nonperturbative treatment [1,2] which has lead to disagreements about the nature and limitations of an EFT expansion in this case. [3,4,5,6,7,8,9] Regularization is needed to handle divergences that arise, but the results are said to depend on the regularization scheme used and the size of the scattering length involved. More generally, it is claimed that the behavior and predictive power expected from a true effective field theory is not exhibited by every regularization method when applied nonperturbatively. [3,4]

Therefore, R. J. Furnstahl and I set out to determine the important features of a nonperturbative EFT[b]. This can be done most clearly by making a side-by-side comparison of the regularization schemes listed in Table 1 using the error analysis advocated by Lepage. [4] This comparison illustrates which schemes behave like a true EFT, [10] as will be seen below. In addition, the differences seen from a comparison with successful phenomenological models for NN scattering such as the Reid potential [11] help determine the importance of a reformulation in terms of an EFT.

[a] Email: jsteele@mps.ohio-state.edu
[b] All the work presented here has been done in collaboration with R. J. Furnstahl. [10]

Table 1: Regularization schemes and their abbreviations used throughout this paper.

name	regularization scheme
CR[G]	Cutoff regularization with gaussian weighting in the potential [4]
DR[$\overline{\text{MS}}$]	Dimensional regularization with modified minimal subtraction [5]
DR[PDS]	Dimensional regularization with power divergence subtraction [12]
dibaryon	DR[$\overline{\text{MS}}$] but with an additional degree of freedom associated with a low-energy bound or nearly bound state [7,13].

2 Comparison Techniques

I first describe how to analyze and compare the different regularization schemes in a way that will allow for a determination of which schemes have the systematics and predictability desired of an effective field theory. Concentrating on S-wave scattering, I will focus only on the short-distance EFT. This general S-wave potential can be written as

$$V(\mathbf{p},\mathbf{p}') = \frac{4\pi}{\Lambda_s^2}\left(c - d\,\frac{\mathbf{p}^2+\mathbf{p}'^2}{2\Lambda_s^2} + e\,\frac{(\mathbf{p}^2+\mathbf{p}'^2)^2}{4\Lambda_s^4} + \ldots\right) , \qquad (1)$$

with a scale Λ_s introduced to make the coefficients c, d, e, ..., dimensionless. There is also a scale Λ implicit in this effective potential that signifies the point above which new degrees of freedom not accounted for in the effective theory begin to contribute to the physics. [4] The factor of $1/4\pi$ picked up by each additional term in the Born series requires a 4π to be factored out in order to render these coefficients natural, [1] *i.e.* of order unity, as discussed further below.

The coefficients are determined order-by-order from matching to the available data. To fit the first n constants in the potential requires at least n points of data. The potential is not a measurable quantity, so instead a scattering observable such as the phase shift $\delta(p)$ is used to determine these constants.

Inserting this potential into the Lippmann-Schwinger equation and specifying a regularization scheme, the resulting amplitude determines the phase shift by one of the following two equivalent relations ($T = -\mathcal{A}$)

$$T(p) = -\frac{4\pi}{Mp}e^{i\delta(p)}\sin\delta(p) , \qquad -\frac{4\pi}{M}\frac{1}{T(p)} = p\cot\delta(p) - ip . \qquad (2)$$

For example, dimensional regularization with modified minimal subtraction

(DR[$\overline{\text{MS}}$]) gives

$$T_{\text{DR}[\overline{\text{MS}}]} = \frac{V(p,p)}{1 + \dfrac{iMp}{4\pi} V(p,p)} \ . \tag{3}$$

The imaginary part of the denominator is linked to the numerator by unitarity. In general, however, the real part of the denominator can be more complicated than in the DR[$\overline{\text{MS}}$] case and consequently dictates the behavior of the scheme near a bound state. This can be seen by calculating the same quantity for dimensional regularization with power divergence subtraction (DR[PDS])

$$T_{\text{DR[PDS]}} = \frac{V(p,p)}{1 + \dfrac{M}{4\pi}(\mu + ip) V(p,p)} \tag{4}$$

which reduces to the DR[$\overline{\text{MS}}$] result for $\mu = 0$. However, the appearance of this additional mass scale is important for a good radius of convergence as will be seen in the next section.

Cutoff regularization is another method for dealing with divergences in which momenta greater than the scale of new physics Λ are explicitly suppressed. This can be implemented by adding a gaussian weight $\exp(-(\mathbf{p}^2 + \mathbf{p}'^2)/2\Lambda_c^2)$ to the potential in Eq. (1) and will be referred to as CR[G]. Although a physically intuitive method, numerical techniques are required to solve this type of regularization. However, one can see the effect of the cutoff by taking a geometric sum of the first two Born terms of the CR[G] method. This just ends up giving Eq. (4) with $\mu = 2\Lambda_c/\pi$. It will be shown below that DR[$\overline{\text{MS}}$] has very different results from both DR[PDS] and CR[G], which can be traced to this difference in the real parts of the T-matrix denominators.

In the left plot of Fig. 1, I show the results from using CR[G] to fit one, two, and three constants in the potential, as compared to the exact S-wave phase-shift for the delta-shell potential,[14] which models the underlying physics and is discussed in detail in the next section. A first glance at the plot shows the approximation to the phase shift improves as more constants in the potential are fit. However, a second look shows that it is very difficult to gather any *quantitative* information from the plot. At what point the curve deviates enough to be considered inaccurate is not clear, and the radius of convergence of the EFT expansion is completely obscure. Furthermore, a simple calculation shows that every term in the momentum expansion of the phase shift contains the scattering length.[5] This means that the error in the phase shift could be numerically sensitive to a large scattering length and contaminate the power counting.

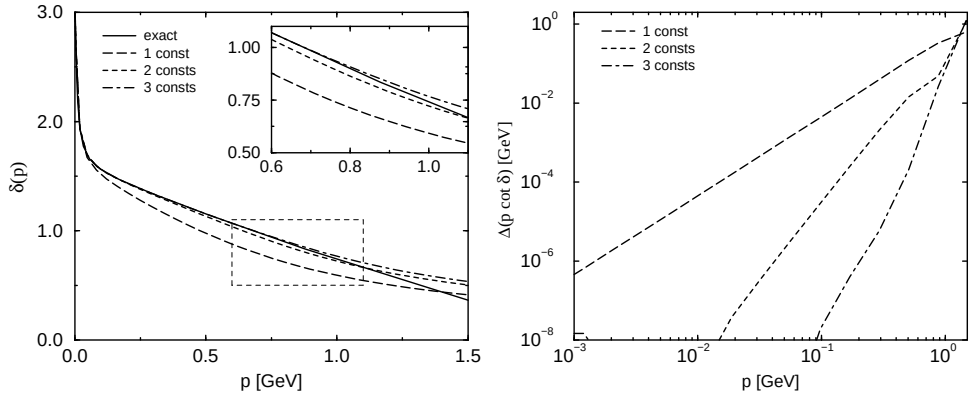

Figure 1: The phase shift $\delta(p)$ (left) and the error in $p\cot\delta(p)$ (right), each plotted as a function of p for the delta-shell potential with a weakly bound state, as discussed in Section 3. The solid line is the exact result and the dashed lines show the CR[G] fit for one, two, and three constants.

This issue is avoided with no loss of generality by plotting the error of $p\cot\delta(p)$ instead:

$$\Delta[p\cot\delta(p)] \equiv |p\cot\delta_{\rm eff}(p) - p\cot\delta_{\rm true}(p)| \ . \tag{5}$$

If the effective field theory follows proper power counting, then this error should improve by two powers of momentum as each additional coefficient in the potential is fixed in Eq. (1). Since a large scattering length is synonymous with a near bound state (or pole) in the amplitude, Eq. (2) shows that this pole is cleanly mapped only to the first constant in a momentum expansion of $p\cot\delta(p)$. It is known from conventional scattering theory that this combination has a well defined expansion in p^2 for short-range potentials known as the "effective range expansion"

$$p\cot\delta(p) = -\frac{1}{a_s} + \frac{1}{2}r_e p^2 + v_2 p^4 + \dots \ , \tag{6}$$

which defines the scattering length a_s and effective range r_e. When long-range potentials are included, Eq. (6) is only valid at low momentum or is even inapplicable. In this case, one must define a modified effective range expansion. [15] Since the effective theory contains the same long-distance physics as the true underlying theory, Eq. (5) can be modified to have a clean momentum expansion. For short range potentials as considered here, Eq. (5) is sufficient.

Plotting the error in $p \cot \delta(p)$ as a function of p on a log-log plot, a straight line is expected with slope given by the dominant (lowest) power of p/Λ in the error. [4] As more constants are included, the slope in this error should increase, signifying the removal of higher powers of p/Λ. The second plot of Fig. 1 clearly demonstrates the order-by-order improvement in the amplitude as more constants are added to the effective potential. With one constant the slope of the error is two, *i.e.*, $\mathcal{O}(p^2/\Lambda^2)$, and increases by two with each additional constant.

3 Illustration with Delta-Shell Potential

In this section, I illustrate the points made above by using EFT techniques with the different regularization methods to systematically describe the "unknown" short-range physics of a specific example. I could use NN scattering data, but it is more convenient to use an exactly solvable potential to serve as data in order to have a clean understanding of what features are important. The delta-shell potential has been used in the past to simulate the large scattering length found in NN scattering. [14] Kaplan used this potential to illustrate the benefits of the dibaryon approach. [7] He found upon considering NN scattering that the inclusion of long-distance pion physics did not change the conclusions. This agrees with the experience of other authors [3,5] that the addition of pions as long-range interactions does not affect the properties of the short-range expansion. The delta-shell potential is therefore a sufficient model for the purposes here.

The potential can be written in terms of the nucleon mass M, the coupling g, and the range of the potential r_0. This short-range potential represents the new physics of the underlying model theory, and so $r_0 = 1/\Lambda$ is taken below,

$$V_{\rm true}(r) = -g\frac{\Lambda}{M}\,\delta\left(r - \frac{1}{\Lambda}\right). \tag{7}$$

It has exactly one bound state for $g \geq 1$ and no bound states for $g < 1$. Scattering with $p > \Lambda$ probes the details of the potential, so one would expect Λ to be the radius of convergence of a well-tuned EFT. The scattering length becomes very large for g near 1, whereas the effective range (and the rest of the terms in the effective range expansion) are of natural size for all g:

$$a_s = \frac{g}{g-1}\,\frac{1}{\Lambda}\,, \qquad\qquad r_e = \frac{2(g+1)}{3g}\,\frac{1}{\Lambda}\,. \tag{8}$$

The scattering length in the ${}^1S_0$ channel of NN-scattering can be modeled by choosing $(g, \Lambda) = (0.99, m_\rho)$. This potential Eq. (7) with different g's will be

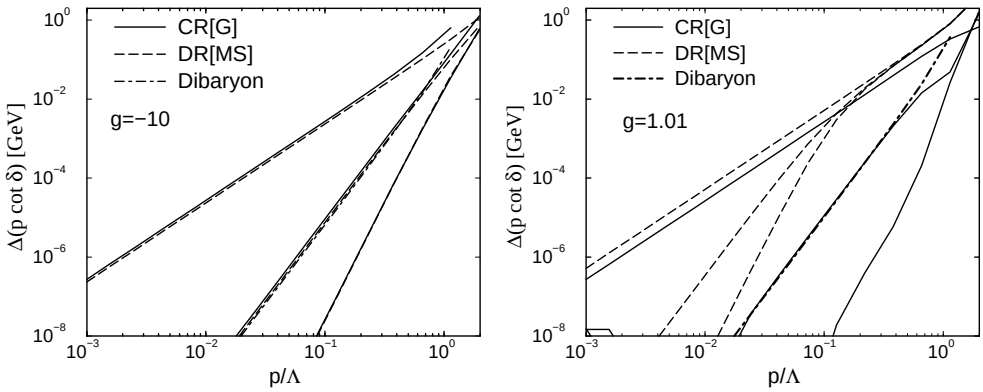

Figure 2: The error in $p\cot\delta(p)$ plotted as a function of p/Λ for a small scattering length without a bound state $g=-10$ and for a large scattering length with a bound state $g=1.01$.

the "laboratory" from which the different regularization schemes are compared. I will also briefly discuss results for actual measured data and the inclusion of pions below.

First, some intuition will be gained by graphically reproducing Kaplan's result that DR[$\overline{\text{MS}}$] has a small radius of convergence if the scattering length is large. From Eq. (8), it can be seen that choosing $g=0.99$ gives a scattering length one hundred times larger than choosing $g=-10$. At the same time, the effect from the presence of a bound state is investigated by taking $g=1.01$. The effective potential is given by Eq. (1) with the mass scale Λ_s associated with the inverse delta-shell radius and the prescription of using DR[$\overline{\text{MS}}$] on all divergent integrals.

The momentum expansion for DR[$\overline{\text{MS}}$] can be shown analytically [5,7] to be $p^2 a_s r_e/2$. This implies using Eq. (8) that the radius of convergence for $g=1.01$ and 0.99 should be roughly 1/10 that of the $g=-10$ case. Fixing the constants in the potential Eq. (1) by matching $p\cot\delta(p)$ produces the results in Fig. 2. The dashed lines show the DR[$\overline{\text{MS}}$] results for one, two, and three constants respectively. Indeed all three lines converge to $p/\Lambda\sim 1$ for $g=-10$ and $p/\Lambda\sim 0.1$ for $g=1.01$. The results for $g=0.99$ fall on top of the $g=1.01$ results and are therefore not shown. This implies the presence of a bound state does not matter, but the size of the scattering length does. It would be difficult to draw these conclusions had only the phase shift itself been plotted (the left plot of Fig. 1). Of course, these results can also be shown analytically for this

Table 2: Effective potential for $g = -10$ (small scattering length) to three different orders in the error $\mathcal{O}(p^n/\Lambda^n)$ for different regularization schemes. $\Lambda a = 1$ for CR[G] and $\mu = \Lambda$ for DR[PDS].

error	DR[$\overline{\text{MS}}$]			DR[PDS]			CR[G]		
order	c	d	e	c	d	e	c	d	e
2	0.758	—	—	8.33	—	—	1.49	—	—
4	0.758	−0.206	—	8.33	−25.0	—	2.67	−1.04	—
6	0.758	−0.206	0.0672	8.33	−25.0	38.2	2.67	−1.58	3.75

Table 3: Effective potential for $g = 1.01$ (large scattering length) to three different orders in the error $\mathcal{O}(p^n/\Lambda^n)$ for different regularization schemes. $\Lambda a = 1$ for CR[G] and $\mu = \Lambda$ for DR[PDS].

error	DR[$\overline{\text{MS}}$]			DR[PDS]			CR[G]		
order	c	d	e	c	d	e	c	d	e
2	84.2	—	—	−0.842	—	—	−1.42	—	—
4	84.2	−5640	—	−0.842	−0.564	—	−0.946	0.842	—
6	84.2	−5640	378000	−0.842	−0.564	−0.152	−0.937	0.618	−0.181

simple model, but the analysis applies much more generally, when part or all of the calculation is done numerically.

The constants c, d, and e are given in Tables 2 and 3. Their values are required to at least 8 digits to produce the accuracy of Fig. 2. The correlation between the naturalness of the constants and the radius of convergence is apparent. The constants for the $g = 1.01$ case are extremely large, reflecting the breakdown of the effective field theory for DR[$\overline{\text{MS}}$] much below the expected scale Λ.

One way to fix this behavior is to introduce the dibaryon. [6,7] This takes the large scattering length into account by explicitly introducing a low-energy s-channel degree of freedom into the effective lagrangian. For $g > 0$ or $g < -1$, the potential can be written as

$$V_{\text{dib.}}(\mathbf{p}, \mathbf{p}') = C - \frac{y^2}{E + \Delta}; \quad C = \frac{2\pi}{M\Lambda}, \quad y^2 = \frac{3\pi\Lambda}{M^2}\frac{1+g}{g}, \quad \Delta = \frac{3\Lambda^2}{2M}\frac{1-g}{g}, \tag{9}$$

with $E = p^2/M$ always kept on-shell. Since there seem to be three constants fit in Eq. (9), one might think the dibaryon will have an error of $\mathcal{O}(p^6/\Lambda^6)$. However, the dibaryon amplitude is only matched to second order [7] in the momentum when deriving the relations in Eq. (9) and indeed shows an error of $\mathcal{O}(p^4/\Lambda^4)$ for the two values of g in Fig. 2 (plotted as the dot-dashed line). The slope and magnitude of the error do not depend on the scattering length,

as expected.

I next repeat the calculations using the cutoff regularization method CR[G] with $\Lambda_c = \Lambda$. There are various ways to numerically solve the Schrödinger equation with a cutoff, but the following procedure is particularly efficient and numerically robust enough to attain the accuracy required here. First, the variable phase method is used to solve for the phase shift. This is a differential equation,

$$\delta'(r) = -\frac{M}{p}\, V(r)\, \sin^2(pr + \delta(r)) \qquad \text{with } \delta(0) = 0 \ , \tag{10}$$

which expresses the change in the phase shift as the potential is built up from zero at $r = 0$ to its full value at $r = \infty$. The boundary condition ensures that the full phase shift given by $\delta(\infty)$ is zero in the absence of a potential and defines the otherwise ambiguous multiple of π in the phase shift. The routine ODE from package ODE [16] was used to solve the differential equation.

Then I use a general method for taking the theoretical error of the EFT into account when matching the constants in the effective potential. After evaluating the combination $p \cot \delta_{\rm eff}(p)$ in the effective theory, it is subtracted from the true result (either data or an exact solution to a model problem) and the difference,

$$\Delta p \cot \delta(p) = \alpha + \beta \frac{p^2}{\Lambda^2} + \gamma \frac{p^4}{\Lambda^4} + \dots \ , \tag{11}$$

is fit to a polynomial in p^2/Λ^2 to as high an order as possible. To obtain the accuracy shown in the plots, a weighted polynomial fit of $\Delta p \cot \delta(p)$ up to $p/\Lambda = 0.1$ was required.

Using a spread of momentum near zero, the polynomial fit should be weighted with both the expected theoretical error in momentum and any additional experimental noise. The resulting coefficients $\alpha, \beta, \gamma, \dots$ are then minimized with respect to variations in the effective potential constants $c, d, e, \dots$ using an optimization code. In practice, this method is more robust and numerically stable than matching the values of $p \cot \delta(p)$ at discrete points to fix the constants. This allows the analysis of Lepage [4] to be extended beyond second order. Also note that such a procedure is needed when matching to data even when the EFT observables can be calculated analytically.

The number of coefficients that can be minimized is given by the number of constants retained in the effective potential. I used DPOLFT from package SLATEC[16] to find the polynomial fit and MINF,[17] which is based on the Powell method, to carry out the minimization. Normal accuracies in minimization using double precision numbers with this method are 10^{-12} or better.

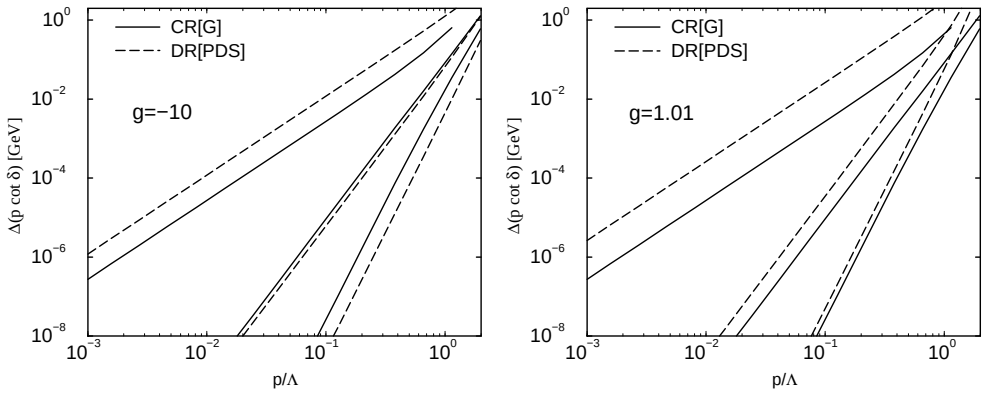

Figure 3: The error in $p \cot \delta(p)$ plotted as a function of p/Λ for a small scattering length without a bound state $g = -10$ and for a large scattering length with a bound state $g = 1.01$.

The solid lines in Fig. 2 show that CR[G] does work regardless of the scattering length. In fact, with $\Lambda_c \sim \Lambda$, the result is just as good as the dibaryon for the same number of constants. The values for the constants are given in Tables 2 and 3, showing they are all natural for both g's (although the third constant is somewhat small for $g = 1.01$).

Note that as more constants are fixed, the lower-order constants are modified. This occurs because even after truncating the potential for the cutoff regularization to a given order, it still contains all orders in p^2 from the gaussian factor. The nonperturbative solution of the Lippmann-Schwinger equation therefore can generate terms of *any* order in p^2/Λ^2. The amplitude itself is matched to the true result order-by-order in the momentum so the power counting of the potential is destroyed. This consequence of the cutoff regularization is not necessarily relevant since the potential is not an observable. It is interesting to note, however, that these modifications are relatively small. This is also true when adding the long distance physics of the pion in fitting to actual NN data as shown in the next section.

In summary, Fig. 2 shows that all regularization schemes considered so far produce useful effective field theories for a small scattering length, but DR[$\overline{\text{MS}}$] fails for large scattering length. A failure of the power counting in powers of p/Λ is reflected in unnatural constants in the potential.

I now turn to the most recently proposed regularization scheme,[12] DR[PDS]. An additional prescription compared to the DR[$\overline{\text{MS}}$] case is an expansion of

observables to the same order in p^2 as the potential Eq. (1). If this is not done, the results are μ dependent, with $\mu = 0$ reproducing DR[$\overline{\rm MS}$] and μ larger than the nucleon mass approaching the CR[G] result in Fig. 2.

When only dealing with a short-range potential as discussed so far, the DR[PDS] prescription reproduces the effective range expansion Eq. (6) by construction. The DR[PDS] results in Fig. 3 are therefore μ independent, but the constants are still μ dependent. I take $\mu = \Lambda$ to compare with CR[G]. This produces natural constants for $g = 1.01$ but somewhat unnatural ones for $g = -10$ as seen in Table 2. This is an accidental consequence of the momentum expansion being in powers of $p^2 r_e/2(\mu - 1/a_s)$, so that for $g = -10$ and $\mu = \Lambda$, Eq. (8) shows the denominator is nearly zero. This implies that the scale μ is not functionally equivalent to the cutoff $1/a$ in CR[G] since it does not always signal the onset of new physics at the scale Λ.

For both large and small scattering length, DR[PDS] does quite well, with a radius of convergence $p/\Lambda \sim 1$. The CR[G] result is better for one constant since the cutoff generates an effective range r_e close to the true result. Overall, DR[PDS] is a convenient method to produce reasonable analytical results, and depending on the problem at hand either CR[G] or DR[PDS] may be suitable. One should note, however, that only DR[PDS] provides a strict diagram by diagram power counting. [12]

Finally, I mention the Reid potential [11] which consists of a sum of Yukawa interactions, with fixed masses chosen as integer multiples of the pion mass, and coefficients that can be varied to fit the data. So for S-waves,

$$V_{\rm Reid}(\mathbf{p},\mathbf{p}') = \frac{c_1}{\mathbf{q}^2 + m_\pi^2} + \frac{c_2}{\mathbf{q}^2 + (3m_\pi)^2} + \frac{c_3}{\mathbf{q}^2 + (5m_\pi)^2} + \dots \qquad (12)$$
$$= {\rm OPE} + \frac{c_2(5m_\pi)^2 + c_3(3m_\pi)^2 + (c_2 + c_3)\mathbf{q}^2}{[\mathbf{q}^2 + (3m_\pi)^2][\mathbf{q}^2 + (5m_\pi)^2]} \ .$$

Combining the Yukawa terms in the second equation generates a numerator that looks like an EFT and a denominator that suppresses large momentum, similar to the cutoff regularization. However, since each term has a different mass, a clear separation scale Λ is not identified. There is also a one-pion exchange (OPE) term which is not important for the short-range physics discussed here.

The original Reid analysis used a global fit and only one adjustable parameter in each channel, for a result with approximately the same error (roughly a few percent of the data) at all momenta. However, the EFT fitting procedure can be applied instead. Using Yukawa masses comparable to Λ should give similar results to CR[G]. Indeed, if the OPE contribution is ignored and a low-momentum fit is done to the constant c_2, the error plot is similar to

the CR[G] result with one constant (Fig. 2). Adding a second short-range Yukawa does as well as CR[G] with two constants, since the Yukawas play off each other to allow the next order error in $\mathbf{q}^2$ to be removed. This interplay becomes increasingly complex at higher orders. Furthermore, the additional mass scales obscure (or smear out) the role of Λ as a scale that separates the known from the unknown physics in effective field theories. Traditional NN potentials such as Reid are well suited for global fits, but systematic predictions with controlled error estimates are more properly analyzed using an effective field theory.

4 Other Observables

I now turn to an investigation of the binding energy. If the EFT is truly reproducing the S-matrix of the underlying theory order-by-order in a momentum expansion, it should reproduce the binding energies and other observables to the same order of accuracy as the phase shifts. I therefore use the binding energy prediction as a consistency check for the candidate effective field theories found so far.

The potentials have already been fit to a given order by the scattering phase shifts above, and I use these potentials without adjustment to solve for the binding energy. This can be done analytically for the DR schemes by finding the poles in the scattering amplitude. The exact binding energy $E_{\rm bind}$ for the delta-shell potential is given by solving the equation

$$\frac{1}{g} = \frac{1-e^{-2\eta}}{2\eta}, \qquad \eta = \frac{\sqrt{ME_{\rm bind}}}{\Lambda}. \tag{13}$$

There is only one bound state to predict in the delta-shell potential, and if it is shallow enough, even the effective range expansion with the values of a_s and r_e can determine its value. A better test is to increase g until $E_{\rm bind}$ is large and on the order of Λ, and use the EFT to determine the accuracy of the binding energy prediction as a function of this variation. If a true radius of convergence is present, the effective field theory should break down for $E_{\rm bind}/\Lambda \sim 1$. The binding energy is 6.48×10^{-2} MeV for $g = 1.01$ but quickly increases to 812 MeV for $g = 2.5$.

The relative error in the binding energy is plotted in Fig. 4. Both CR[G] and DR[PDS] show the clear power counting behavior and proper radius of convergence expected from a true effective field theory. This gives a graphical verification that the errors in the binding energy really do follow power counting rules. I have checked that the same behavior is seen when plotted as a function of the average momentum $\sqrt{\langle p^2 \rangle}/\Lambda$. The dibaryon result also follows

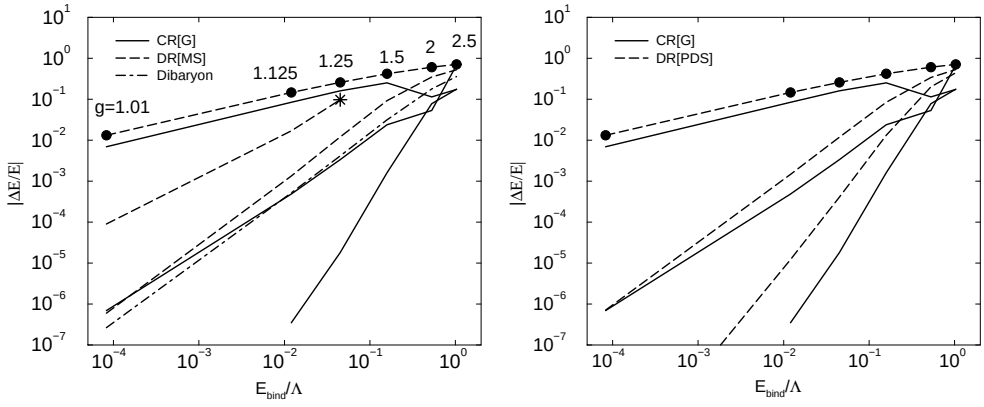

Figure 4: The error in the binding energy for the candidate effective field theories for representative values of g from 1.01 to 2.5. The star signifies the absence of real binding energies for DR[$\overline{\rm MS}$] with two constants at the values of $g > 1.25$ considered.

the expected error scaling. In contrast, the deficiencies of DR[$\overline{\rm MS}$] regularization seen for the phase shifts are manifested here as binding energies that do not follow the EFT error scaling, improving to a lesser degree than expected. In addition, for values of $g > 1.25$ with two constants, the DR[$\overline{\rm MS}$] S-matrix shows no bound state with a real energy.

Therefore, these results show that most regularization procedures demonstrate the characteristics of a systematic predictive effective field theory. The fit of more and more constants in the effective potential improves the predictive power order-by-order in the momentum expansion. The radius of convergence of the EFT is independent of the scattering length and is given by the scale where new physics enters.

This test can be taken further by looking at moments of the bound state wavefunction, such as $\langle r^2 \rangle$. Preliminary results are shown in the left plot of Fig. 5 for one and two constants. Going to third order is not productive here because the effective operator r^2 changes [4] due to the operator product expansion at this order in $1/\Lambda^2$. A systematic improvement of the expectation value is nevertheless seen for one and two constants. The radius of convergence does not look optimal, but this is merely an illusion since CR[G] with one constant does slightly better than anticipated for large $E_{\rm bind}/\Lambda$, as seen from Fig. 4.

Finally, it would be ideal to apply the present analysis to real data for

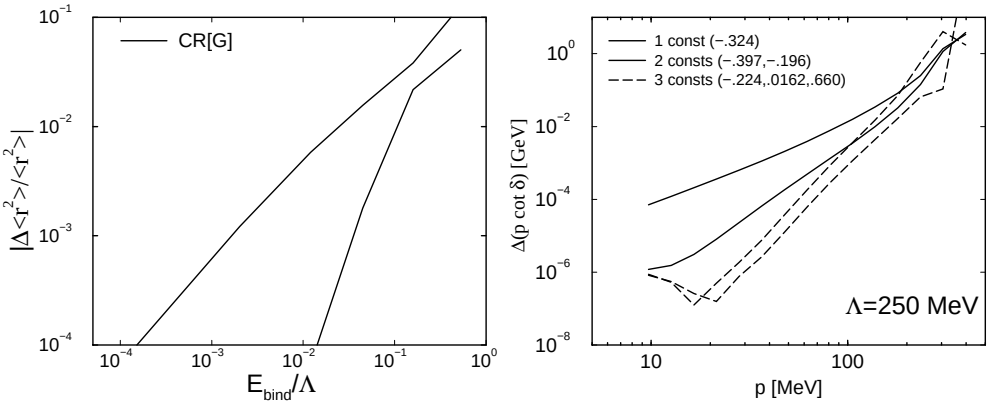

Figure 5: The left plot shows the error from the bound state moment $\langle r^2 \rangle$ in the delta-shell potential. The right plot shows the result for one, two, and three constants in CR[G] when fit to the ${}^1S_0$ NN scattering data from Nijmegen. [18]

NN scattering. Using the data from the Nijmegen phase shift analysis, [18] I have taken the theoretical error in the EFT analysis with CR[G] and the experimental uncertainties into account in constructing the right plot of Fig. 5. Since two-pion physics was not included in the analysis, the cutoff was taken near the $2m_\pi$ threshold ($\Lambda = 250$ MeV). The one and two constant results show the systematic improvement and nice radius of convergence expected from above. However, the uncertainty in the long distance physics blurs the three constant result given by the range between the two dotted lines. This must be looked at in more detail to achieve a better precision fit.

5 Conclusion

I have presented results [10] showing how the error analysis suggested by Lepage [4] can be applied to compare cutoff regularization, two forms of dimensional regularization, and the dibaryon approach in the context of nonperturbative, nonrelativistic effective field theories. This analysis focuses on a key signature of EFT behavior: the systematic scaling of errors with momentum or energy.

New numerical procedures [10] allow for an analysis to third order and beyond in the EFT expansion, which is necessary to obtain a clear graphical determination of the radius of convergence for a given observable. Such an analysis is required for a systematic fit to data regardless of the regularization

scheme.

It is found that all of the regularization methods except for dimensional regularization with modified minimal subtraction are consistent with basic features expected from a useful effective field theory:

- Each additional order in the potential leads to a systematic improvement in the amplitude.
- The radius of convergence for this improvement, when optimized, is dictated by the scale of new physics.
- Other observables are predicted with the same accuracy as the amplitude at each successive improvement.

These results are consistent with the analysis of van Kolck that, with proper resummations, any effective field theory for short-range interactions is equivalent to an effective range expansion to the same order. [13]

The CR[G] and DR[PDS] regularization schemes are each suitable for developing effective field theories of many-nucleon systems. In future work both schemes will be used in extending this fitting procedure and error analysis to nuclear matter.

Acknowledgments

This work was supported by the National Science Foundation under Grants No. PHY–9511923 and PHY–9258270.

References

1. S. Weinberg, *Phys. Lett.* B **251**, 288 (1990); *Nucl. Phys.* B **363**, 3 (1991).
2. U. van Kolck, Ph.D. thesis, U. Texas, Aug. 1993; C. Ordonez, L. Ray, and U. van Kolck, *Phys. Rev. Lett.* **72**, 1982 (1994); *Phys. Rev.* C **53**, 2086 (1996).
3. S. R. Beane, T. D. Cohen, and D. R. Phillips, *Nucl. Phys.* A **632**, 445 (1998); D. R. Phillips and T. D. Cohen, *Phys. Lett.* B **390**, 7 (1997); D. R. Phillips, S. R. Beane, and T. D. Cohen, *Ann. Phys.* **263**, 255 (1998); K. A. Scaldeferri, D. R. Phillips, C.-W. Kao, and T. D. Cohen, *Phys. Rev.* C **56**, 679 (1997).
4. G. P. Lepage, "How to Renormalize the Schrodinger Equation," nucl-th/9706029.
5. D. B. Kaplan, M. J. Savage, and M. B. Wise, *Nucl. Phys.* B **478**, 629 (1996).

6. M. Luke and A. V. Manohar, *Phys. Rev.* D **55**, 4129 (1997).
7. D. B. Kaplan, *Nucl. Phys.* B **494**, 471 (1997); P. F. Bedaque and U. van Kolck, "Nucleon-Deuteron Scattering from an Effective Field Theory," nucl-th/9710073; P. F. Bedaque, H.–W. Hammer, and U. van Kolck, "Effective Theory for Neutron-Deuteron Scattering: Energy Dependence," nucl-th/9802057.
8. K. G. Richardson, M. C. Birse, and J. A. McGovern, "Renormalization and Power Counting in Effective Field Theories for Nucleon-Nucleon Scattering," hep-ph/9708435.
9. J. Gegelia, "Chiral Perturbation Theory Approach to NN Scattering Problem," nucl-th/9802038, 1998.
10. J. V. Steele and R. J. Furnstahl, "Regularization Methods for Nucleon-Nucleon Effective Field Theory," nucl-th/9802069.
11. R. V. Reid, *Ann. Phys.* **50**, 411 (1968).
12. D. B. Kaplan, M. J. Savage, and M. B. Wise, "A New Expansion for Nucleon-Nucleon Interactions," nucl-th/9801034; "Two-nucleon Systems from Effective Field Theory," nucl-th/9802075.
13. U. van Kolck, "Nucleon-Nucleon Interaction and Isospin Violation," hep-ph/9711222.
14. K. Gottfried, *Quantum Mechanics*, (Benjamin, Reading, MA, 1979).
15. J. R. Bergervoet *et al.*, in *Quarks and Nuclear Structure*, ed. K. Bleuler, (Springer-Verlag, New York, 1984).
16. These numerical routines can be found online at the Guide to Available Math Software website http://gams.nist.gov/
17. M. J. D. Powell, *Comp. J.* **7**, 155 (1964); W. I. Zangwill, *Comp. J.* **10**, 293 (1967).
18. Partial wave data and Papers of the Nijmegen University group can be found at http://nn-online.sci.kun.nl/.